Hydrodynamic - Acoustic Filtering of a Supersonic Under-expanded Jet

C. Pérez Arroyo, G. Daviller, G. Puigt, and C. Airiau

1 Introduction

The noise perceived in the aft-cabin for an aircraft at cruise conditions is mainly due to the turbofan jet. The pressure mismatch between the ambient air and the secondary stream of a turbofan engine leads to the formation of (diamond-shaped) shock-cells. These series of expansion and compression waves interact with the vortical structures developing in the mixing layer of the jet. This interaction process generates intense noise components on top of the turbulent mixing noise, which makes supersonic jets noisier than their subsonic counterparts [15]. The result is a broadband shock-cell associated noise (BBSAN), radiated mainly in the forward direction, which impinges on the aircraft fuselage and it is then transmitted to the cabin.

In this paper, the shock-cell noise generated by an axisymmetric under-expanded single jet is investigated using Large-Eddy Simulations (LES). The paper addresses in a first term, the code characteristics and simulation setup and procedure. The second part of the paper focuses on the application of acoustic-hydrodynamic filtering and its impact on the cross-correlation in the near-field.

C. Pérez Arroyo · G. Puigt
Centre Européen de Recherche et de Formation Avancée en Calcul Scientifique, 42 Avenue Gaspard Coriolis, 31057 Toulouse Cedex 01, France, e-mail: {cparroyo,guillaume.puigt}@cerfacs.fr

G. Daviller · C. Airiau
Institut de Mcanique des Fluides de Toulouse, UMR 5502 CNRS/INPT-UPS, Alle du professeur Camille Soula, 31400 Toulouse, France, e-mail: {guillaume.daviller,christophe.airiau}@imft.fr

2 Numerical Formulation

The full compressible Navier-Stokes equations in skew-symmetric formulation are solved using the Finite Volume multi-block structured solver ***elsA*** (Onera's software [4]). The spatial scheme is based on the well-known implicit compact finite difference scheme of 6th order of Lele [7], extended to Finite Volumes by Fosso *et al.* [6]. The above scheme is stabilized by the compact filter of Visbal & Gaitonde [18] that is also used as an implicit subgrid-scale model for the present LES. Time integration is performed by a six-step 3rd order Runge-Kutta DRP scheme of Bogey and Bailly [3].

3 Simulation Setup and Procedure

Time-dependent simulations are presented of a contoured convergent nozzle with exit diameter $D = 38.0mm$ and a modeled nozzle lip thickness of $t = 0.125D$. The nozzle is operated under-expanded at the stagnation to ambient pressure ratio $p_s/p_\infty = 2.27$. The modeled exit and ambient conditions match those in the experimental set-up of André [1]. The Reynolds number, Re, based on the jet exit diameter is 1.2×10^6 and the fully expanded jet Mach number is $M_j = 1.15$.

The numerical computation is initialized by a RANS simulation using the Spalart-Allmaras turbulence model [13]. The RANS solution is wall resolved in the inner and outer sections of the nozzle with a $y^+ < 1$. Once mesh convergence is achieved, the LES run is then initialized from the RANS simulation. The inner part of the nozzle is removed from the LES simulation and the RANS nozzle exit conservative variables are imposed, as [14, 19, 11, 12, 9, 10]. In addition, no inflow forcing is used.

The computational domain used for the LES simulation extends $40D$ in the axial direction and $7D$ in the radial direction. The mesh consists in 75×10^6 cells with $(1052 \times 270 \times 256)$ cells in the axial, radial and azimuthal directions respectively. The maximum expansion ratio between adjacent cells achieved in the mesh is less than 4%.

Non-reflective boundary conditions of Tam and Dong [16] extended to three dimensions by Bogey and Bailly [2] are used in the exterior inlet as well as in the lateral boundaries. The exit condition is based on the characteristic formulation of Poinsot and Lele [8]. Furthermore, sponge layers are coupled around the domain to attenuate exiting vorticity waves. Due to the fact that the interior of the nozzle is not modeled, no inflow forcing is applied at the exit of the nozzle to avoid parasite noise.

The simulation runs for 120 non-dimensional time units ($\hat{t} = tD/C_\infty$) in order to reach statistically independent results.

4 Hydrodynamic - Acoustic filtering

The acoustic component of a jet can be filtered from the hydrodynamic one in the near-field, where the mean velocity is zero using the methodology shown by Tinney and Jordan [17]. The original pressure signal $p(x_p,t)$ is transformed into the wavelength - frequency domain by

$$p(k_x,\omega) = \int\int p(x_p,t)W(x_p)e^{-j(k_x x_p+\omega t)}dx_p dt, \tag{1}$$

where the reference coordinate x_p is such that it is located outside the jet verifying a null mean velocity throughout the new coordinate. $W(x_p)$ is a weight function used to smooth the signal at the ends of the axis. An acoustic fluctuation generated by a noise source inside the jet will be propagated outside the jet at the ambient sound speed c_∞. However, the acoustic perturbation will be propagated at a supersonic speed $c_x^2 = c_\infty(2df + c_\infty)$ in the x_p coordinate system, where d is the perpendicular distance from the axis to the noise source and f is its frequency. The subsonic and supersonic components, i.e. the hydrodynamic and acoustic components can be recovered from the transformed signal obtained by Eq. 1 using only the ranges $p(k_x > \omega, \omega < k_x c_\infty)$ and $p(k_x < \omega, \omega > k_x c_\infty)$ respectively as:

$$p_{sub}(x_p,t) = \int p(k_x > \omega, \omega < k_x c_\infty)e^{-j(k_x x_p+\omega t)}dk_x d\omega, \tag{2}$$

$$p_{super}(x_p,t) = \int p(k_x < \omega, \omega > k_x c_\infty)e^{-j(k_x x_p+\omega t)}dk_x d\omega. \tag{3}$$

The filtering has been applied to the supersonic under-expanded jet near-field over several lines in order to obtain a two-dimensional field of the pressure perturbation. Figure 1a shows the original pressure perturbations of a snapshot where the jet is represented by the axial velocity. It can be compared with the filtered hydrodynamic and acoustic components in figures 1b and 1c respectively. The filtering allows the hydrodynamic component to be clearly visible and the acoustic component to gain in detail specially near the jet, where the hydrodynamic perturbations are more intense.

The importance of the hydrodynamic-acoustic filtering is further noted when spatio-temporal cross-correlations of the filtered pressure are carried out in the near-field. Figures 2a, 2b and 2c show the cross-correlation between one point located at $[x/D = 0, y/D = 3]$ and an array located at $y/D = 1$ with an inclination of 5°, following the expansion of the shear layer.

The shock-cell noise is found around $x/D = 4$ with a cross-correlation of 0.38. When the filtering is applied, the cross-correlation peak increases up to 0.41 and it becomes clearer downstream of the end of the potential core ($x/D > 9$). The filtering improves the cross-correlation specially downstream where the hydrodynamic components have the same general direction as the acoustic waves. Figures 3a, 3b and 3c now focus the cross-correlation on the point located at $[x/D = 15, y/D = 3]$ and

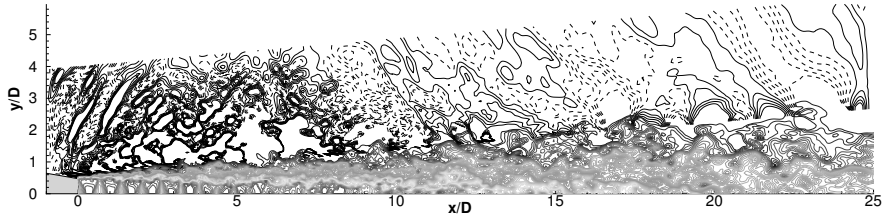

Fig. 1a Pressure perturbations of the original flow, $-150Pa < p \leq 150Pa$.

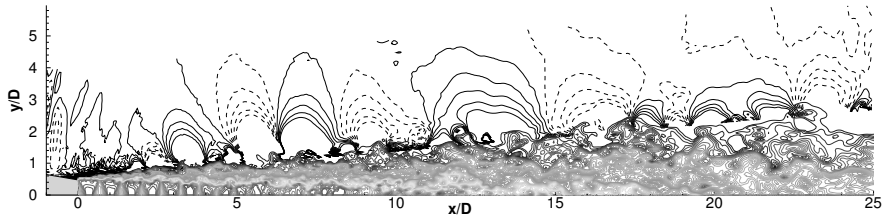

Fig. 1b Pressure perturbations of the subsonic (hydrodynamic) component, $-150Pa < p \leq 150Pa$.

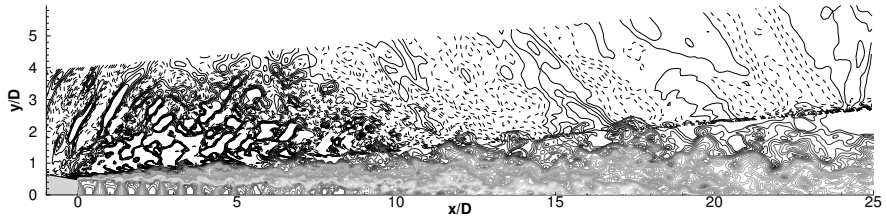

Fig. 1c Pressure perturbations of the supersonic (acoustic) component, $-150Pa < p \leq 150Pa$.

the above-mentioned array. At this position, the original cross-correlation shown in figure 3a differs completely from the acoustic component shown in figure 3c. The original signal is clearly dominated by the hydrodynamic component shown in 3b adopting the same shape. The mixing noise of the large turbulent structures is mostly generated at the end of the potential core and radiated at 30° [15]. The cross-correlation of the acoustic component agrees with the theory showing a high correlation up to this location, with a convective velocity at the speed of sound.

6 Conclusions

The hydrodynamic - acoustic filtering of the near-field of a supersonic under-expanded axisymmetric jet has been carried out. Post-processing techniques such as spatio-temporal cross-correlations are affected by the filtering achieving different conclusions depending on whether or not the filtering is used. The shock-cell noise and the mixing noise of the large turbulent structures have been identified in figures 2c and 3c respectively. This approach looks very promising to study in depth the shock-cell noise mechanism.

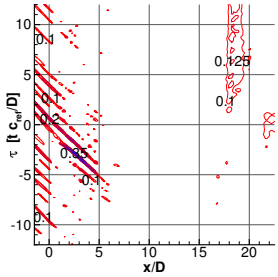

Fig. 2a Spatio-temporal pressure cross-correlation of the complete original signal at $x/D = 0.0$.

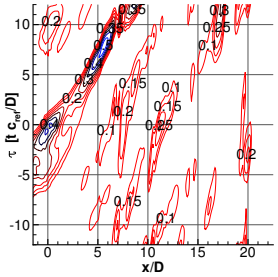

Fig. 2b Spatio-temporal pressure cross-correlation of the hydrodynamic component at $x/D = 0.0$.

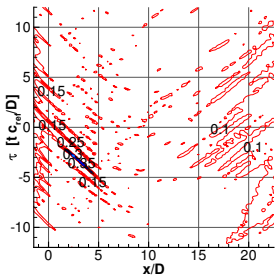

Fig. 2c Spatio-temporal pressure cross-correlation of the acoustic component at $x/D = 0.0$.

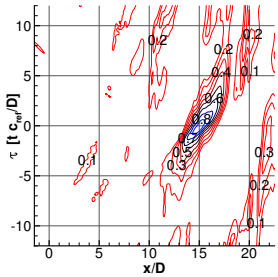

Fig. 3a Spatio-temporal pressure cross-correlation of the complete original signal at $x/D = 15.0$.

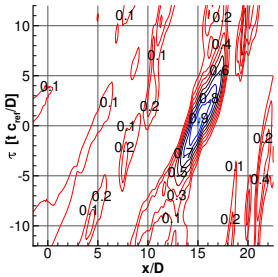

Fig. 3b Spatio-temporal pressure cross-correlation of the hydrodynamic component at $x/D = 15.0$.

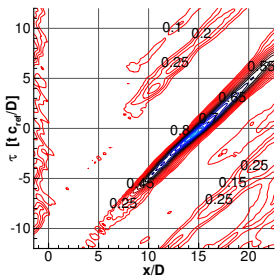

Fig. 3c Spatio-temporal pressure cross-correlation of the acoustic component at $x/D = 15.0$.

The simulation of a co-axial nozzle where the secondary jet is under-expanded and other filtering techniques will be applied in the future.

Acknowledgments

This research project has been supported by a Marie Curie Initial Training Networks (ITN) AeroTraNet 2 of the European Community Seventh Framework Programme (FP7) under contract number PITN-GA-2012-317142 that aims to generate a ready to use model for shock-cell noise characterization.

This work was performed using HPC resources from GENCI-[CCRT/CINES/IDRIS] (Grant 2015-[x20152a6074]).

References

1. André, B.: Etude expérimentale de l'effet du vol sur le bruit de choc de jets supersoniques sous-détendus. (2012)
2. Bogey, C., Bailly, C.: Three-dimensional non-reflective boundary conditions for acoustic simulations: far field formulation and validation test cases. Acta Acust., **88**, 463–471 (2002)
3. Bogey, C., Bailly, C.: A family of low dispersive and low dissipative explicit schemes for flow and noise computations. J. Comput. Phys., **194**, 194–214 (2004)
4. Cambier, L.; Heib, S., Plot, S.: The Onera elsA CFD software: input from research and feedback from industry. Mech. & Ind., **14**, 159–174 (2013)
5. Farassat, F., Succi, G. P.: The prediction of helicopter rotor discrete frequency noise. American Helicopter Society, Annual Forum, 38th, Anaheim, CA, May 4–7, Proceedings.(A82-40505 20-01) Washington, DC, **1**, 497–507 (1982)
6. Fosso-Pouangué, A.; Deniau, H.; Sicot, F., Sagaut, P.: Curvilinear Finite Volume Schemes using High Order Compact Interpolation. J. Comput. Phys., **229**, 5090–5122 (2010)
7. Lele, S.: Compact finite difference schemes with spectral-like resolution. J. Comput. Phys., **103**, 16–42 (1992)
8. Poinsot, T.J., Lele, S.K.: Boundary Conditions for Direct Simulations of Compressible Viscous Flows. J. Comput. Phys., **101**, 104–129 (1992)
9. Schaupp, C.; Sesterhenn, J., Friedrich, R.: On a method for direct numerical simulation of shear layer/compression wave interaction for aeroacoustic investigations. Comput. Fluids, **37**, 463–474 (2008)
10. Schulze, J.; Sesterhenn, J.; Schmid, P.; Bogey, C.; de Cacqueray, N.; Berland, J., Bailly, C.: Numerical simulation of supersonic jet noise. Num. Sim. of Turbulent Flows & Noise Generation, **104**, 29–46 (2009)
11. Shur, M.; Spalart, P., Strelets, M.: Noise prediction for increasingly complex jets. Part I: Methods and tests. Int. J. Aeroacoustics, **4**, 213–246 (2005)
12. Shur, M. L.; Spalart, P. R.; Strelets, M. K., Garbaruk, A. V.: Further steps in LES-based noise prediction for complex jets. AIAAP 44th AIAA Aerospace Sciences Meeting and Exhibit, Reno, Nevada, AIAA Paper 2006-485, **485** (2006)
13. Spalart, P., Allmaras, S.: A one-equation turbulence model for aerodynamic flows. AIAA Paper 92-0439, 30th Aerospace Sciences Meeting and Exhibit, Reno, Nevada (1992)
14. Suzuki, T., Lele, S. K.: Shock leakage through an unsteady vortex-laden mixing layer: application to jet screech. J. Fluid Mech. **490**, 139-167 (2003)
15. Tam, C. K.: Supersonic jet noise. Annu. Rev. of Fluid Mech., **27**, 17–43 (1995)
16. Tam, C., Dong, Z.: Radiation and outflow boundary conditions for direct computation of acoustic and flow disturbances in a nonuniform mean flow. J. Comput. Phys., **4**, 175–201 (1996)
17. Tinney, C.; Jordan, P., others: The near pressure field of co-axial subsonic jets. J. Fluid Mech. **611**, 175–204 (2008)
18. Visbal, M., Gaitonde, D.: On the Use of Higher-Order Finite-Difference Schemes on Curvilinear and Deforming Meshes. J. Comput. Phys., **181**, 155–185 (2002)
19. Viswanathan, K.; Shur, M.; Strelets, M., Spalart, P. R.: Numerical Prediction of Noise from Round and Beveled Nozzles. Turbulent Flow and Noise Generation, EUROMECH Colloquium Marseille, France, **467** (2005)